

Wright State University

CORE Scholar

Biomedical, Industrial & Human Factors
Engineering Faculty Publications

Biomedical, Industrial & Human Factors
Engineering

1997

Corrosion Fatigue Crack Growth Behavior of Aircraft Materials

Tarun Goswami

D. W. Hoepfner

Follow this and additional works at: <https://corescholar.libraries.wright.edu/bie>



Part of the [Biomedical Engineering and Bioengineering Commons](#), and the [Industrial Engineering Commons](#)

CORROSION FATIGUE CRACK GROWTH BEHAVIOR OF AIRCRAFT MATERIALS

T. Goswami¹ and D. W. Hoepfner

Quality and Integrity Design Engineering Center

Department of Mechanical Engineering

University of Utah, Salt Lake City, UT 84112.

ABSTRACT

The effects of test parameters on the corrosion fatigue crack growth behavior of structural materials have been examined in this paper. Test parameters such as stress ratio, frequency, hold time, temperature, pH level of the media, and other parameters are known to alter the corrosion fatigue crack growth rates in structural materials. Numerous laboratory test variables that affect the crack growth and/or corrosion growth rates, which in an operating environment of an aircraft are not characterized, are reviewed. A summary of such information may help determine the inspection intervals of the new and aged airplanes, perform the inspections, and develop repair procedures against corrosion and corrosion fatigue damages.

Keywords: aluminum alloys, corrosion fatigue, crack growth, stress ratio, 3.5%NaCl.

¹ Presently at Damage Tolerance and Fatigue Group, Cessna Aircraft Company, 2617 South, Hoover Road, Wichita, KS 67215-1200, also at Department of Mechanical Engineering, Wichita State University, KS 67260-0035, USA.

1 INTRODUCTION

Corrosion and corrosion fatigue of aircraft structural materials is very important since corrosion and corrosion fatigue has emerged as one of the potential failure mechanisms in military and commercial fleets. The aircraft usage parameters such as stress, time in each flight segment, environment, corrosivity of the media, temperature and material parameters such as joint characteristics and presence of corrosion in the joints are known to a very limited extent, life assessments and growth rate predictions of corrosion and cracks are very difficult. Quantitative discretization of these parameters is a complex issue since operating conditions change with respect to the individual aircraft and their individual flights. Therefore, research in corrosion fatigue crack growth behavior in aircraft structural materials within the extremity of test parameters and failure mechanisms are very important to simulate and correlate the service failure with laboratory tests. Since the crack or corrosion detection depends upon the crack size or percentage material loss respectively, selection of inspection intervals must be made with extreme care. Joint characteristics, fretting induced microscopic cracks aided by corrosion, linking by multiple site fatigue damage (MSFD) and growth of such cracks are known to a limited extent¹⁾ that they will grow at a faster rate than "long" cracks; crack growth equations under such situations are unknown.

Local dissolution in a material causes corrosion. Local dissolution, passivation and repassivation characteristics of the material determines the rate of corrosion. The corrosion rate can be enhanced by the pH level of the media²⁾ and the chloride ion concentrations³⁾. Test parameters such as load, temperature, strain rate or frequency,

presence of hydrogen and other parameters interact with localized dissolution and passivation characteristics in a material may accelerate the corrosion rates. Interactions among the electrochemical parameters, mechanical parameters, material parameters, time and favorable texture may cause either embrittlement or cracking, growth of which is determined by localized conditions by either corrosion, or when mechanical parameters interact; by corrosion fatigue. The synergisms of various processes in the corrosion fatigue crack growth behavior in aircraft structural materials are not very well understood as there are several potential mechanisms. These parameters alter the aging characteristics of materials when exposed to service conditions. Figure 1 shows the corrosion fatigue crack growth behavior in a 2024-T3 alclad fuselage panel material exposed to nearly

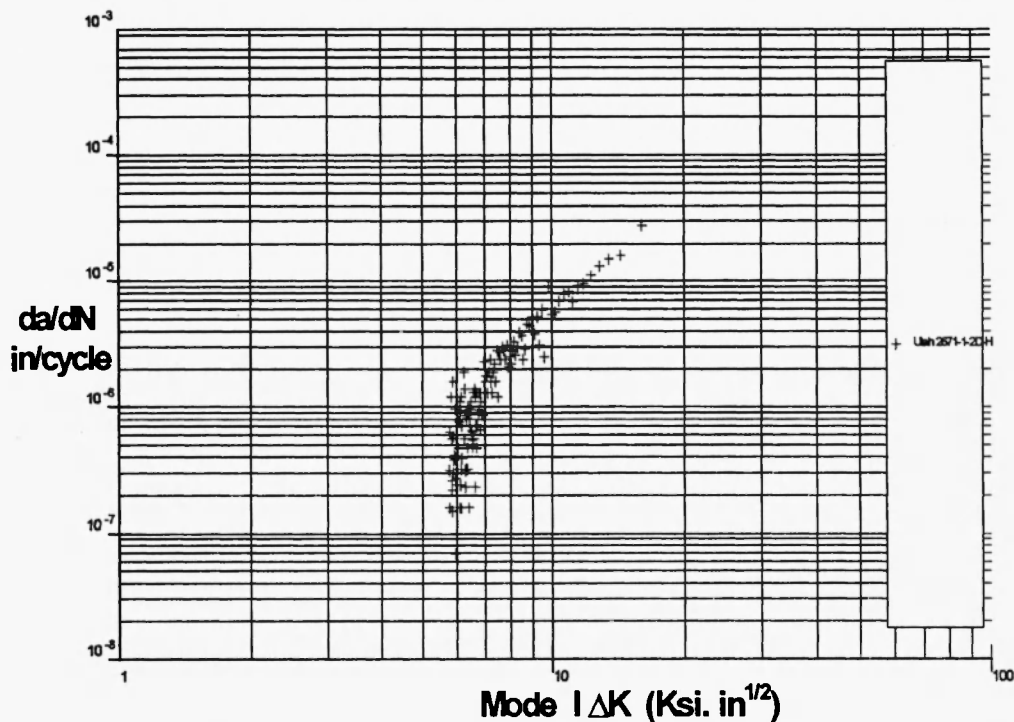


Fig. 1. Corrosion fatigue crack growth behavior of a service exposed 0.06 inch plate tested under high humidity (Conversion factor: 1in.=25.4 mm and 1Ksi-in^{1/2}=1.081MPa m^{1/2}).

26000 hours during 30 years in military service tested under high humidity and at stress ratio; 0.1. The scatter in the data shows that the crack growth rate is indescribable by a power equation under corrosion fatigue.

Fatigue crack growth rates vary in the presence of water in the environment or water vapor pressure, under which a sigmoidal trend in the crack growth rate data is exhibited⁴⁾.

The environmental sensitivity of a material can be altered by proper selection of test parameters such as crack size, frequency, stress ratio and material parameters such as microstructure and composition. However, in an aircraft the growth of "small" cracks from the joints and the parameters that alleviate environmental sensitivity can not be altered. Early work reported by Hoepfner and Hylar⁵⁾ show that fatigue life in 2024-T351 and 7075-T6 aluminum alloys improved with exposure in vacuum of nominally 10^{-6} mm Hg. With the increase in the exposure time in vacuum the fatigue life improved further.

The effort presented herein this paper was directed toward the study of crack growth behavior in aircraft structural materials as influenced by material/environmental/load/time interactions. Sustained load conditions were evaluated on the corrosion fatigue crack growth behavior in the materials which experience sustained loading, for example, that result from an aircraft on the ground with the weight resting on the landing gear for an extended period of time. Therefore, materials studied in this paper were based on the following considerations:

1. the materials are representative of those used in applications such as aircraft wings, fittings, attachment and landing gear component,

2. materials selected represent the major three aerospace materials namely; aluminum, titanium and steel, and
3. materials selected represent that are used and exist on the fleets at the present time.

The effect of corrosion fatigue test parameters in the crack growth behavior is discussed below.

2 MATERIALS AND TESTING:

The materials studied together with the test matrix employed are summarized in Table 1:

Due mainly to the volume of data that are associated with the above materials it may not be possible to present data, but, this paper will discuss critically the crack growth behavior under different test conditions. Interested reader is recommended references for more details⁽⁶⁻⁹⁾.

2.1 Load Sequence Parameters for Test Matrix:

The crack growth tests were conducted in air and other environments for the following three major conditions discussed below:

2.1.1 Continuous fatigue crack growth tests:

Crack growth tests were conducted under continuous fatigue conditions. Table 2 describes the materials and other details investigated.

2.1.2 Sustained load fatigue crack growth tests:

A limited number of sustained load crack growth (SLCG) tests were conducted; a summary of which is provided in Table 3.

Table 1. Summary of materials, alloy types and test conditions examined.

Materials	Alloy types	Test conditions	Environment	Applications
Aluminum alloys	2024 T-351	Trapezoidal and conjoint cycles	air and 3.5% NaCl.	wing and skin applications
	2324- T39	same	same	
	7075-T651	same	same	
	7150-T651	same	same	
	2024-T851	sustained load CG and FCG	high humidity and 3.5% NaCl	
	2124-T851	Fretting corrosion	air and 3.5% NaCl	
Titanium alloys	Ti-6Al-4V (RA)	sustained load CG and FCG	high humidity, 3.5% NaCl and sump water	used as fittings attachments doublers etc.
	Ti-6Al-4V (β A)	Sustained load CG and FCG	high humidity, 3.5% NaCl and sump water.	
	Ti-6Al-6V-2Sn (STOA)	fatigue crack growth	humid air and 3.5% NaCl	
Steel	18Ni-Mar-aging Steel	Sustained load crack growth and FCG	high humidity and 3.5% NaCl	landing gear applications

Table 2: Summary of continuous fatigue test conditions.

Material	Test type	specimen type	Stress ratio	frequency	dry air	high humidity	3.5% NaCl	sump water
2024-T851	FCG	3/4" WOL ¹	0.1	0.1, 1, 2, 10, 20 Hz		most tests	13 tests	
		PTC ²						
		CCT						
18 Ni Maraging steel	FCG	WOL	0.1	0.1, 1 and 10 Hz		one test	3 tests	
Ti-6Al-6V- 2SN (STOA)	FCG	WOL and CCT	0.1 and 0.5	0.1, 1 and 10 Hz	2 tests	9 tests	12 tests	
Ti-6Al-4V (RA)	FCG	WOL, PCT and CCT	0.1 and 0.5	0.1, 1 and 10 Hz	1 test	11 tests	12 tests	6 tests
Ti-6Al-4V beta annealed	FCG	WOL and PCT	0.1 and 0.9	0.1, 1 and 10 Hz	4 tests		6 tests	4 tests

¹ WOL: wedge opening load specimen configuration.

² PTC: Part through cracked specimen geometry.

Table 3: Summary of sustained load test parameters employed.

Material	Test type	specimen type	Stress ratio	frequency	dry air	high humidity	3.5% NaCl	sump water
2024-T851	SLCG	CT				one test	one test	
18Ni Maraging steel	SLCG					2 tests	3 tests	
Ti-6Al-6V-2Sn (STOA)	SLCG	CT				2 tests	2 tests	2 tests
Ti-6Al-4V (RA)	SLCG	CT				2 tests	2 tests	2 tests
Ti-6Al-4V Beta annealed	SLCG	WOL					one test	one test

2.1.3 Ripple fatigue crack growth tests:

Conjoint major-minor waveforms were used to investigate the ripple fatigue crack growth (RFCG) behavior in fatigue and corrosion fatigue conditions in a number of aluminum alloys. A summary of test parameters utilized is tabulated in Table 4.

Tests were conducted on 2024-T351, 2324-T39, 7075-T651 and 7150-T651 aluminum alloys. The CT specimens were machined such that crack growth occurred in T-L orientation.

Table 4: Summary of ripple fatigue crack growth test parameters employed.

Test type	specimen type	Major Stress ratio	Minor stress ratio	Frequency major	Frequency minor	amplitude ratio	cycle ratio
RFCG	CT	0.1	0.5, 0.9	0.2Hz	20.Hz	0.56-0.11	100
RFCG	CT	0.1	0.5-0.9	0.2 Hz	20 Hz	0.56-0.11	25

2.2 TEST PROCEDURE:

All the tests outlined in the Tables 2-4 were in accordance with standard procedure described in ASTM E 399-72 and ASTM E 647-91. For the PTC specimens the stress intensity was computed from the following equation:

$$K_I = 1.1 (P/A) \pi^{1/2} a/Q \quad (1)$$

where P is the load, A is the specimen gross area, a is the crack depth and Q is Irwin plasticity and shape correction factor¹⁰⁾.

The stress intensity for the WOL specimens were calculated by the following equation:

$$K_I = (C_3 P) / (B \cdot a^{1/2}) \quad (2)$$

where details of analyzing these specimens are outlined in the paper by Novak and Rolfe¹¹⁾. For the CCT specimens the stress intensity solution was calculated by the following equation:

$$K_I = P \{ \pi^{1/2} c \sec (\pi c/w) \} / (WB) \quad (3)$$

where c is half the total crack length and w is the width of the panel. Other terms have specific meanings described in ASTM E 399 and 647 respectively.

Sustained load crack growth tests were conducted by pre-cracking the specimens in laboratory air at a stress ratio of 0.1 and a frequency of 10 Hz. The specimens were then placed in a static creep frame, the environment added and load applied. Stress intensity solution recommended in ASTM 399 was used. After a specified time specimens were pulled to failure monotonically and fracture surface studied for the crack growth under sustained loading condition⁶⁾.

3 RESULTS AND DISCUSSION:

The results are discussed for the three groups of tests conducted in this section.

3.1 Continuous fatigue crack growth behavior:

The crack growth rates in the case of 2024-T851 were comparable under test variables such as environment, frequency, orientation, stress ratio and microstructural variables. No significant effect of environment or test frequency in 3.5% NaCl solution was observed. Different specimen sizes produced a slight change in the slope of the crack propagation rate versus stress intensity range data. The samples tested at very high gross stresses showed delamination in the plane parallel to the plate surface at the higher nominal stresses and mode I ΔK values resulting in slight retardation in the crack growth rates. This behavior was expected due mainly to the surface conditions which usually are overworked and constituent particles are often broken as a result of rolling. The stress ratio (0.1 and 0.5) influenced the CGR within the extreme condition of mode I ΔK values

in that at the higher values the maximum stress intensity in the load cycle became a significant percentage of the fracture toughness and at the values of the mode I ΔK where the crack growth rate was below 10^{-6} in. per cycle. However, in a 3.5% NaCl solution and 20 Hz frequency the R=0.5 produced faster crack growth rates at lower mode I ΔK ranges than other environments tabulated in Table 2. A general trend of shifting the data upward with the increase in R from 0.1 to 0.5 was by a factor of one to five. The scatter in the data ranged within this envelope with a change in the environment and frequency. The environmental effects seen in Fig. 2 also found in the literature which was more pronounced at the lower levels of cyclic amplitudes of mode I ΔK . In 2024-T3 tested in a 3.5% NaCl within the range of mode I ΔK from 3.5 to 9 ksi in^{1/2} the CGR varied from 20 to one. In other alloys namely; 7075-T6 and 7178-T6 the environmental effect is not as prominent^{4, 12)}. This behavior was argued due to lower cyclic rates where time dependent corrosion interacted with fatigue. On the contrary, with the increase in the frequency, time for the corrosion attack is reduced substantially, thereby lowering the crack growth rates. An empirical equation for the environmental adsorption effects in fatigue crack propagation was proposed by Achter¹³⁾ as follows:

$$(da/dn)_c = 4.87 \times 10 P/\nu \quad (4)$$

where left hand side of the equation denotes the cyclic crack growth rates in inch per cycle, P is the water vapor pressure and ν the frequency. This equation separates the regimes where a cross-over in the CG behavior under the dry air and other environments should occur. The values obtained by this equation for the transition in the environmental

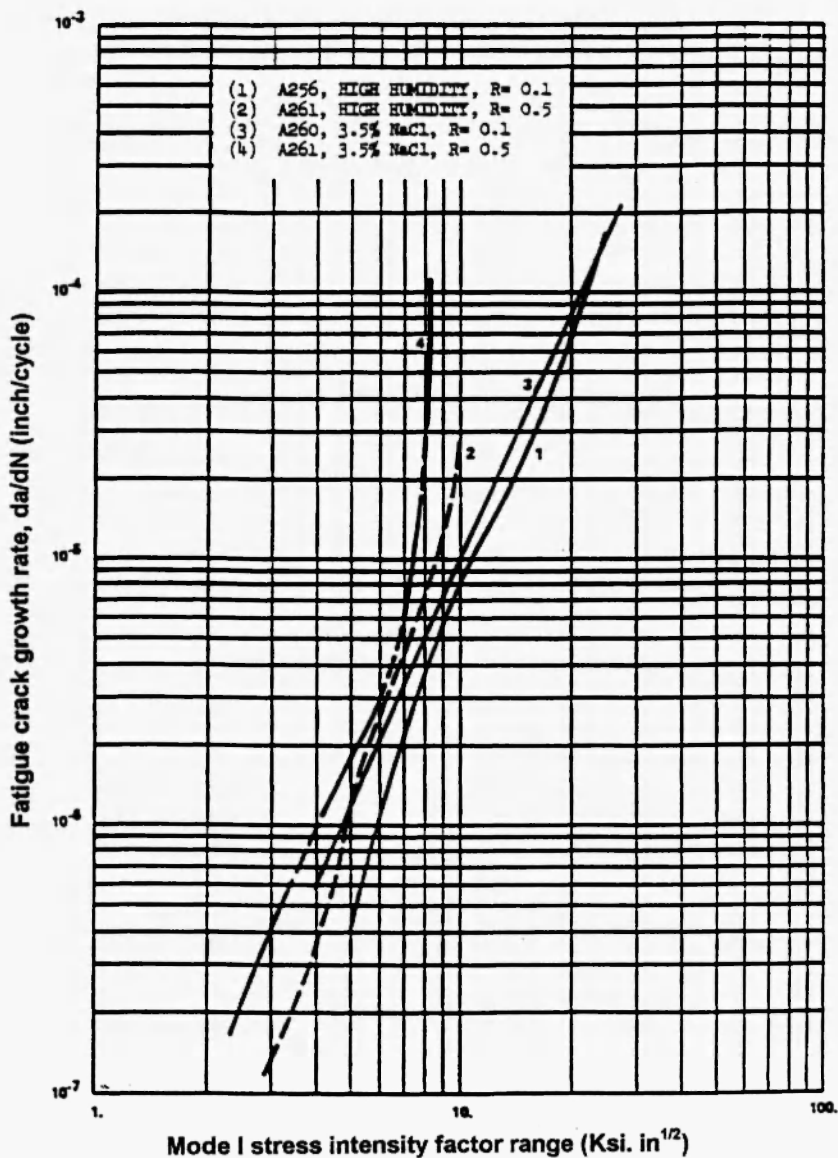


Fig. 2. Effect of stress ratio for 3/8 inch 2024-T851 CCT specimens under 20Hz, WR orientation (Conversion factor: 1 in. = 25.4 mm and 1Ksi in^{1/2} = 1.081MPa m^{1/2}).

CGR and mode I ΔK curve within the frequency range from 0.1 to 20 Hz appeared to be at the range of 10 ksi in^{1/2} and 10⁻⁶ in per cycle, this also conforms to the materials investigated and that found in the literature^{4, 12}.

The fracture surface appeared to be a mixture of ductile striations, limited cleavage and faceted fracture. However, striations were detected only above a critical value of mode I ΔK range. In (Reference 12) striations were found in mild environments (dry air, wet air, and distilled water) beyond the mode I ΔK range of 5 ksi in^{1/2}, in that fine ductile striation networks were observed. Striations were resolved in this study at mode I ΔK of nearly 7.6 ksi in^{1/2} in both humid and 3.5%NaCl solution, where a limited amount of corrosion found together with secondary cracking, cleavage of second phases and traces of oxides filling the crack. With the increase in the mode I ΔK range, striation spacing increased and more pronounced cleavage with step wise transgranular fracture mode observed.

The maraging steel exhibited a gradual increase in the CGR with the decrease in the frequency from 10Hz to 0.1 Hz in 3.5% NaCl environment. The CGR increased at a particular frequency and environment at a higher mode I ΔK ranges in Fig. 3. In a range of mode I ΔK from 10 to 55 ksi in^{1/2} the CGR varied in a factor of 2 to 10. A similar trend in the crack growth behavior was observed in the case of 9Ni-4Co-0.3 C steel¹⁴⁾ where at 0.1 Hz frequency the CGR was found faster than that of 1Hz. The fracture surface appearance contained fine striations, however, as the environment changed to 3.5% NaCl secondary cracking associated intergranular failure⁶⁾. These features were more dominant in 3.5% NaCl solution.

In the case of Ti-6Al-6V-2Sn in (STOA) condition exhibited a gradual increase in the CGR in the intermediate range of mode I ΔK in 3.5% NaCl solution when the frequency was 10Hz. With a decrease in the frequency from 10 to 1 and 0.1 Hz the CGR rapidly

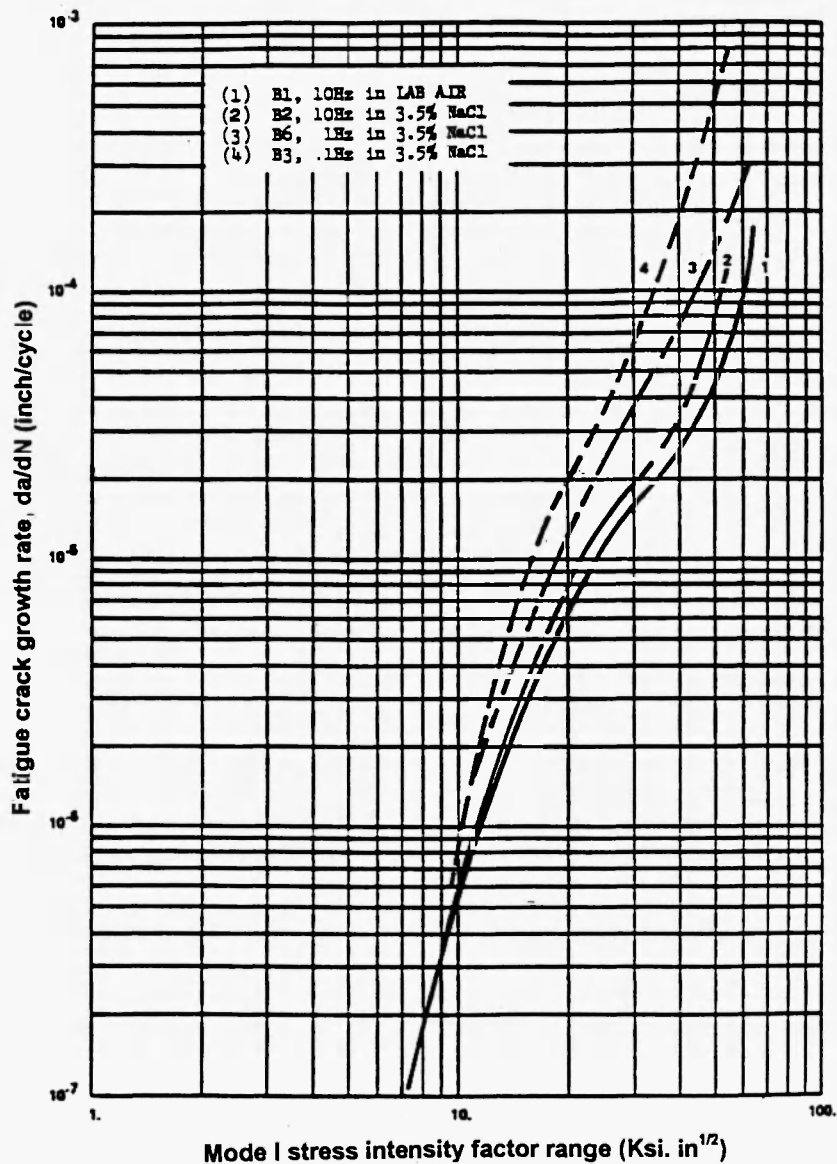


Fig. 3. Effect of frequency for one inch 18Ni-Maraging steel (250 Grade) WOL specimens under R = 0.1, WR orientation (Conversion factor: 1 in. = 25.4 mm and 1Ksi in^{1/2} = 1.081MPa m^{1/2}).

increased to an order of magnitude than that of CGR in air at 10 Hz. A range in the mode I ΔK , in which the crack growth rates rapidly increased was found to be from 10 to 17 Ksi in^{1/2} for most Ti-6Al-6V-2Sn in STOA condition. Different specimen thickness produced

different crack growth rate in different environments was due mainly to the transition behavior where lower rates were as a result of plane stress fracture. Increasing the humidity from 10% to 90% enhanced the CGR at 0.1Hz observed within the intermediate range of mode I ΔK from 10 to 40 ksi in^{1/2} in Fig. 4.

The stress ratio has a similar effect on Ti-6Al-6V-2Sn in STOA condition that observed in the case of 2024-T851 aluminum alloy. With the increase in the R from 0.1 to 0.5 under high humidity (90%) the crack growth rates increased either at the higher side of mode I ΔK range or at the lower range of mode I ΔK where CGR increased a factor of three. In other environments and frequency ranges the scatter was not considerable.

Fractographic results indicated secondary cracking at the higher CGR when the frequency was reduced. The extent of cracking in the coarse alpha increased as the growth rates increased to instability. At the region of instability severe sub-surface secondary cracking occurred which were not connected to the main crack. The crack propagation was by means of transgranular cleavage in the fine acicular alpha phase along the interface of the coarse alpha-beta regions. The features observed under corrosion fatigue in this titanium alloy was also reported by Cowgill et al¹⁵⁾, for stress corrosion of Ti-8Al-1Mo-1V where secondary cracking along alpha-beta interface and in the coarse alpha occurred. Fatigue crack growth and fractographic features in α - β titanium alloys have been extensively researched in references¹⁶⁻¹⁸⁾.

Titanium alloy 6Al-4V in a recrystallized and annealed (RA) condition exhibited a similar trend that observed in the case of Ti-6Al-6V-2Sn under STOA. As the frequency

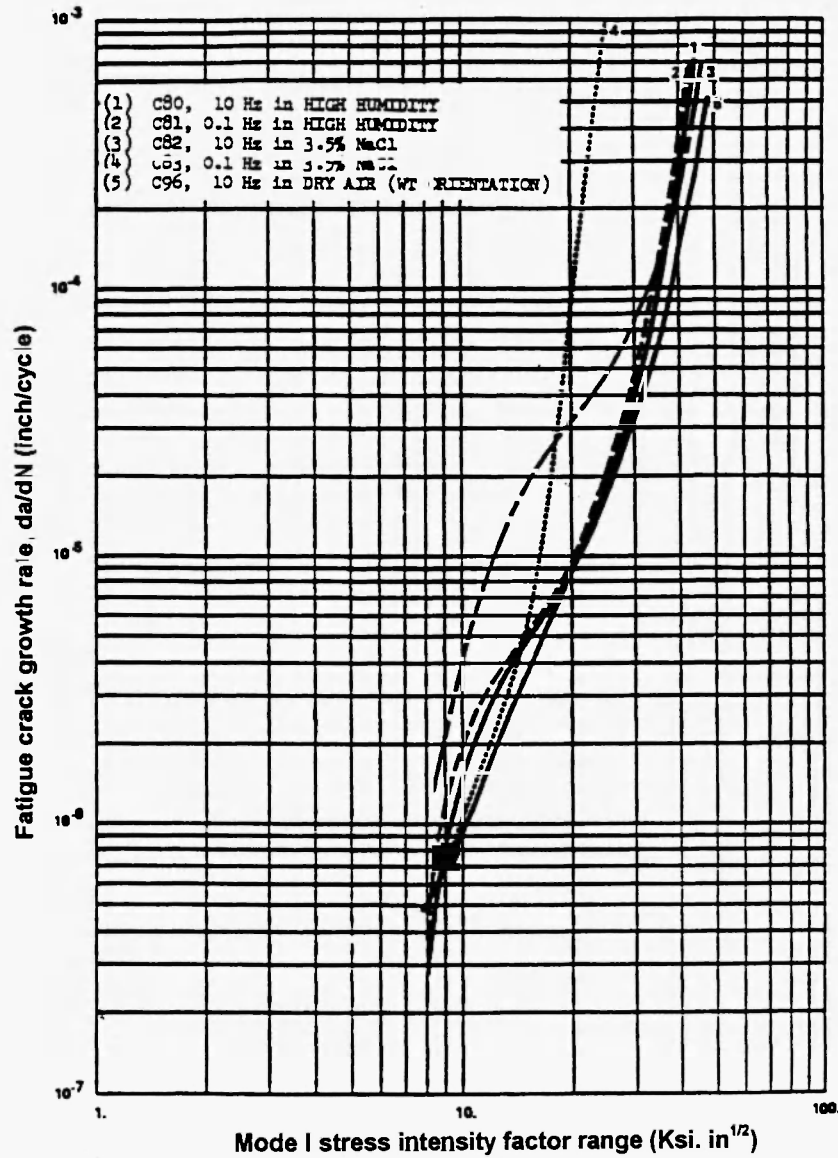


Fig. 4. Fatigue crack propagation results for 3/8 inch Ti-6Al-6V-2Sn (STOA) PTC specimens, R=0.1, RT orientation (Conversion factor: 1 in. = 25.4 mm and 1Ksi in^{1/2} = 1.081MPa m^{1/2}).

decreased from 10 to 1 Hz the CGR increased a factor of 4 and 10 respectively in air 3.5% NaCl. At 0.1 Hz the rapid CGR noted in the Ti-6Al-6V-2Sn under STOA was also observed in Ti-6Al-4V under RA condition at mode I ΔK range of 16 ksi in^{1/2}. The sump

tank water was less aggressive only at lower frequency (10 and 1Hz) ranges the effects of sump tank water was found equivalent to that of 3.5% NaCl at lower frequency levels of 0.1 Hz or less. Different specimen geometries produced different CGR in different environments where thickness was found causing a transition in plane stress fracture and lower CGR. Under different environments the range of mode I ΔK changed from 10 to 16 ksi in^{1/2} beyond which the CGR enhanced in Fig. 5.

Effects of stress ratio from 0.1 to 0.5 was found consistent to that observed for 2024-T851 aluminum alloy and Ti-6Al-6V-2Sn (STOA). At R=0.5 the 10 Hz curves in high humidity and 3.5% NaCl solution showed a significant increase in the CGR at high and low mode I ΔK levels when compared to R = 0.1. This effect was found less significant within the intermediate range of the CGR curve. Beyond the range of $9 > \text{mode I } \Delta K \leq 15$ ksi in^{1/2} no effect of stress ratio occurred. In other environments namely, high humidity and 3.5% NaCl the CGR decelerated at the higher ranges of mode I ΔK .

Fractographic investigations from before the instability region revealed striation, ductile rupture and cleavage. The fatigue striation spacing increased as the CGR increased, with increase in the cleavage and secondary cracking. The increasing amount of cleavage corresponded to the large jump in CGR at a relatively low mode I ΔK .

In a Ti-6Al-4V under beta annealed condition showed a similar behavior related to CGR that in 3.5% NaCl CGR increased with decreasing frequency in Fig. 6, however, the magnitude of the effect was observed to be much smaller than other two titanium alloys. The fracture surface morphology was quite similar to that observed for other two alloys except that fatigue striations associated stepped appearance with fluted dimples between

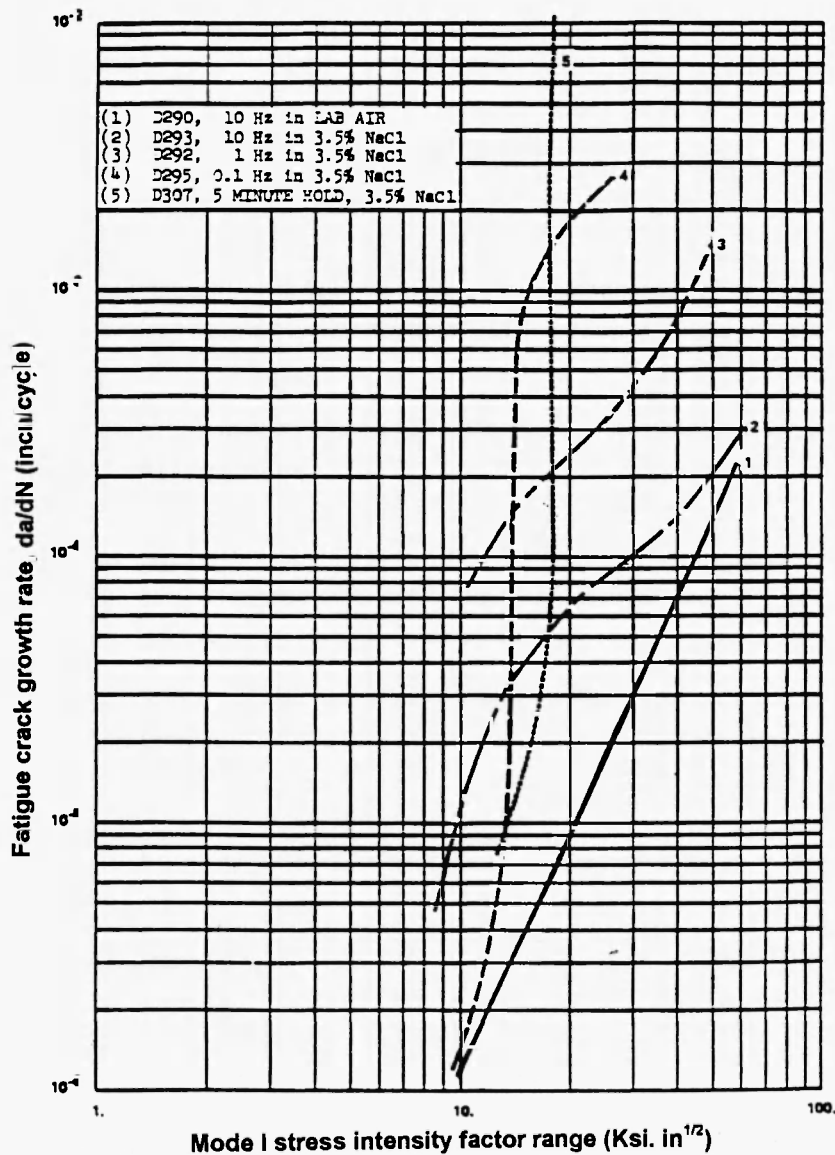


Fig. 5. Effect of frequency for 3/8 inch Ti-6Al-4V (RA) WOL specimens under R = 0.1 in WR orientation (Conversion factor: 1in. = 25.4 mm and 1Ksi in^{1/2} = 1.081MPa m^{1/2}).

steps, characteristics of trans-alpha fracture in a beta processed material, were observed.

3.2 Sustained load fatigue crack growth tests:

Sustained load CGR in aluminum alloy 2024-T851 was found negligible or no effect at all

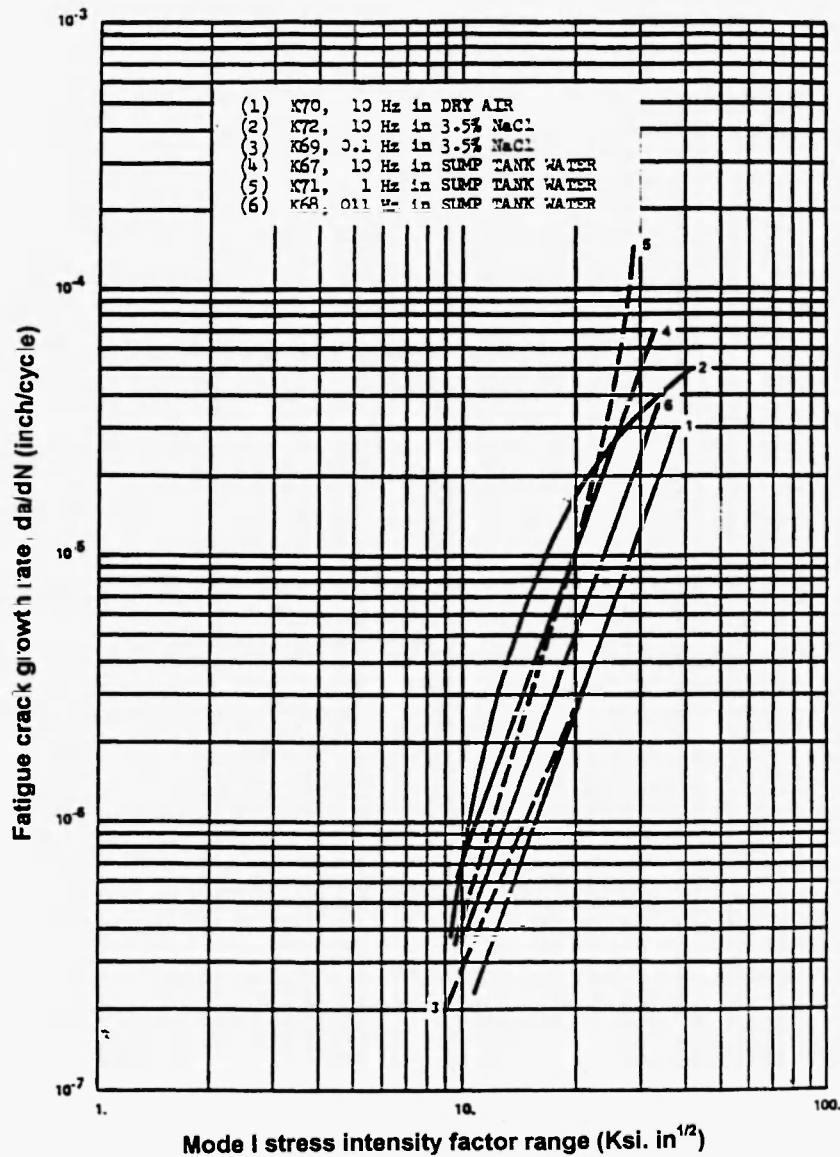


Fig. 6. Trends in the corrosion fatigue crack growth behavior in sump tank water and 3.5% NaCl solution for 5/8 inch Ti-6Al-4V (Beta) WOL specimens, R=0.1 in WR orientation (Conversion factor: 1 in. = 25.4 mm and 1Ksi in^{1/2} = 1.081MPa m^{1/2}).

with the time of exposure from 5 hours to 120 hours. No sub-surface and surface crack growth occurred in this alloy in the environments tabulated in Table 2. However, in a

sister program¹⁴⁾ with 7075-T651 aluminum alloy the stress corrosion effect was found significant at all environments and orientations, in which no apparent threshold stress intensity factor was found below which the SCC would not occur in Fig. 7. The CGR

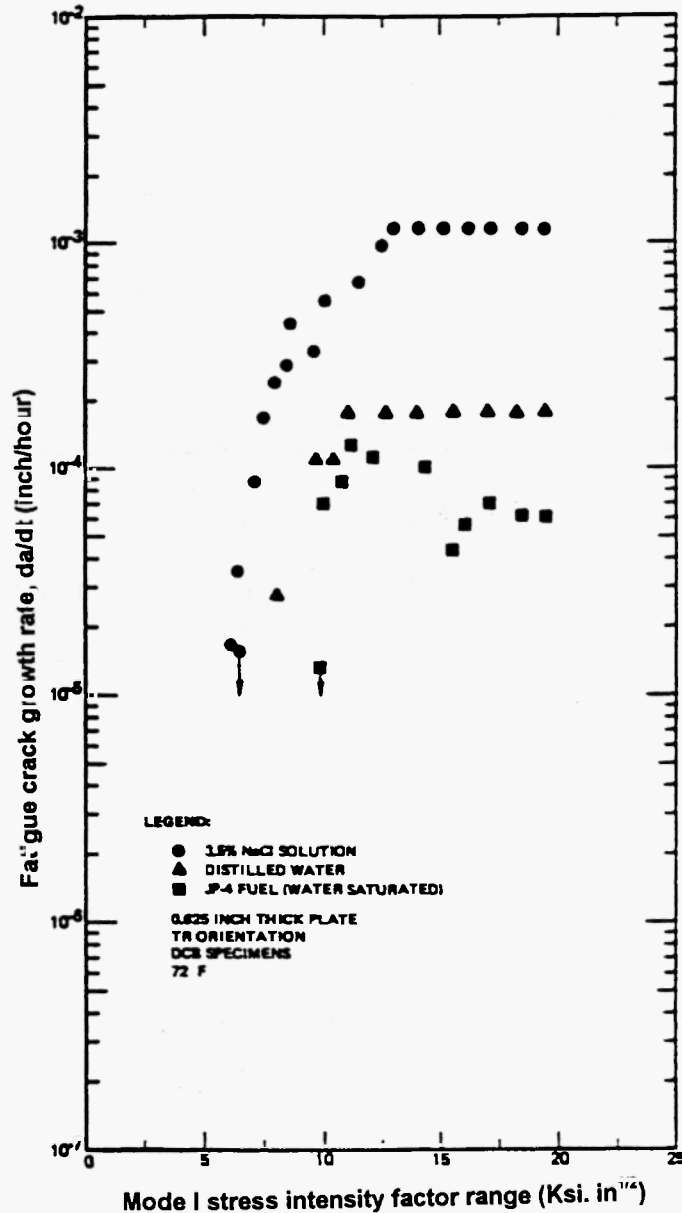


Fig. 7. Stress corrosion cracking velocity data for 7075-T651 aluminum alloy (Reference 14) (Conversion factor: 1 in. = 25.4 mm and $1\text{Ksi in}^{1/2} = 1.081\text{MPa m}^{1/2}$).

became very small at mode I ΔK levels approaching the apparent threshold values, at such point, tests were terminated after nine months since specimens became too corroded¹⁴⁾. For 7475-T651 alloy the effect was more pronounced as above mode I ΔK 12.5 ksi in^{1/2} SCC rates in the 7475-T651 were faster than 7075-T651, below this range the effect was not much different for the two alloys in 3.5% NaCl solution¹⁴⁾.

A limited number of tests were conducted for maraging steel to examine the effect of exposure time in 3.5% NaCl solution to determine the threshold of sustained load crack growth, however, crack growth was observed in the tests conducted. Most specimens exhibited surface and subsurface crack propagation with a small amount of crack front bowing. Exposure to 3.5% NaCl caused a higher CGR than the exposure in humid air. The CGR in 3.5% NaCl solution appear to be a function of stress intensity level, the rate increasing with increasing stress intensity in Fig. 8. Similar to the observation made for 7075-T3 alloy, no threshold value was found for this maraging steel. For the steel, 9Ni-4Co-0.3C the SCC behavior where the crack velocity increased with the time was observed in distilled water and JP-4 fuel¹⁴⁾.

In titanium alloy 6Al-6V-2Sn in STOA condition exhibited SCC in humid air, 3.5% NaCl solution and sump tank water. In all three environments CG occurred below the K levels where failure occurred. In most cases subsurface than on the surface resulting in significant bowing for most specimens. In 3.5% NaCl solution for a specimen 0.001 inch of surface crack accompanied a subsurface crack growth of 0.123 inch. Therefore, subsurface crack growth measurements becomes meaningful for such material where fracture occurred in all the cases above 30 ksi in^{1/2}. The humid air environment was least

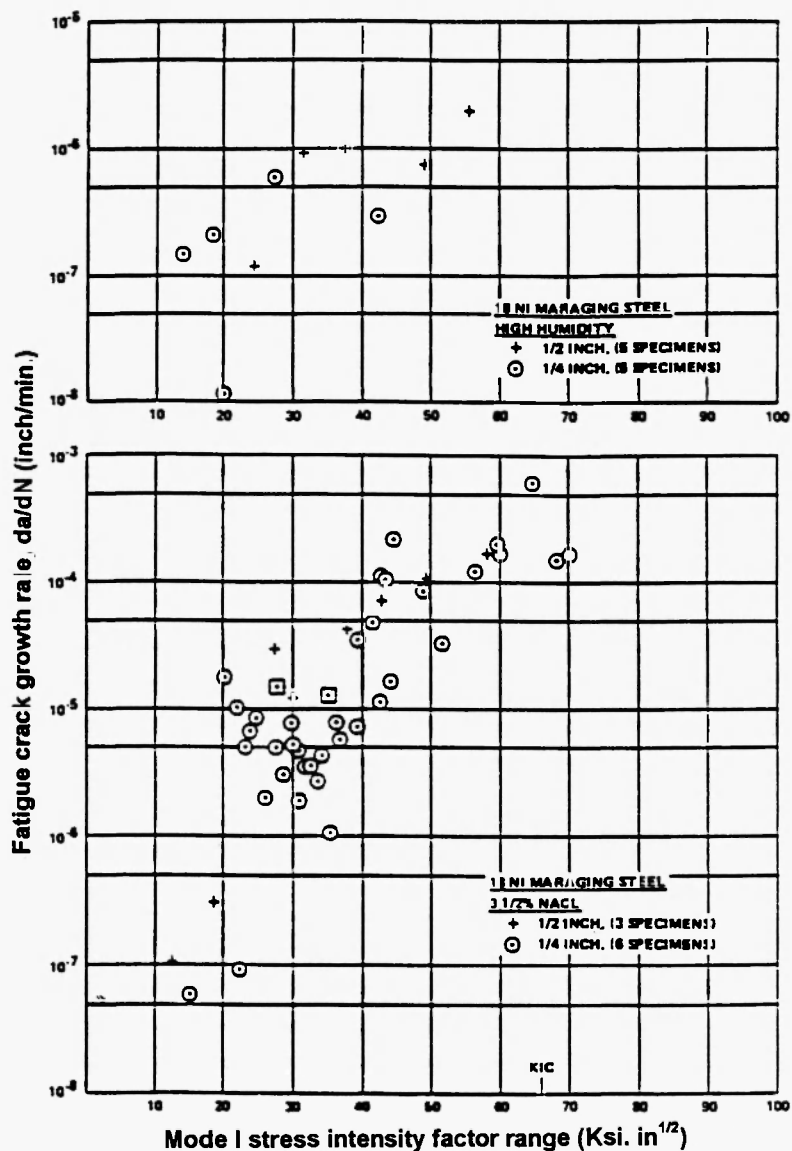


Fig. 8. Stress corrosion crack growth rate behavior of 18Ni-Maraging steel (250 Grade) CT specimens in WR orientation (Conversion factor: 1 in. = 25.4 mm and 1Ksi in^{1/2} = 1.081MPa m^{1/2}).

severe, where sump tank water was next and the 3.5% NaCl solution was found to be most severe shown in Fig. 9. In the case of Ti-6Al-4V beta annealed condition also exhibited subsurface cracking. A CGR of 10⁻⁶ in per cycle was noticed at K values as low

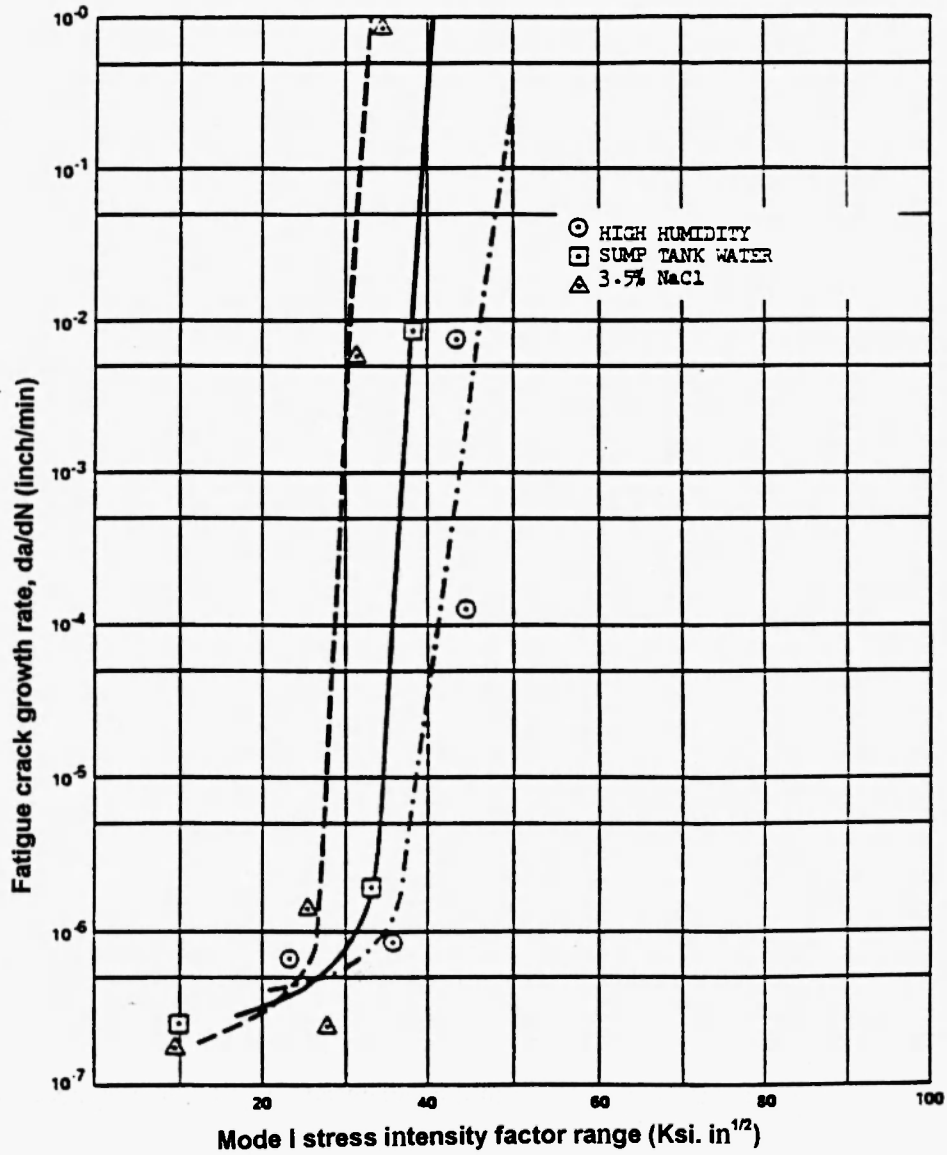


Fig. 9. Stress corrosion crack growth rate for 3/8 inch Ti-6Al-6V-2Sn (STOA) plate material (Conversion factor: 1 in. = 25.4 mm and 1Ksi in^{1/2} = 1.081MPa m^{1/2}).

as 10 ksi in^{1/2}. In RA condition, a similar trend; that is the crack growth rates increased with the increase in the exposure time, was observed. Crack growth was more severe subsurface than on the surface resulting in severe bowing in many cases.

3.3 Ripple fatigue crack growth tests:

Two terms have been investigated in the literature¹⁹⁾ to influence the CGR behavior under ripple or conjoint major-minor cycles are cycle ratio, i.e., the number of minor cycles per major cycle and amplitude ratio (Q) which is a ratio of stress intensity range of the minor loading to the stress intensity range of the major loading. The CGR for four materials listed in Table 1 are found to behave in a similar fashion which showed that as the amplitude ratio increased the CGR increased, however, with the increase in amplitude ratio and the cycle ratio the CGR increased for these materials²⁰⁻²¹⁾.

In 3.5% NaCl solution, at lower amplitude ratio of 0.11 the ripple cycles had little or no effect on the CG behavior of 2024-T351, however, an increase in the CGR was observed only when the amplitude ratio was increased with the increase in the cycle ratio. Alloy 2324-T39 behaved in a similar manner that of 2024-T351. The 7xxx series alloys also exhibited a similar trend, in which the CGR in 7150-T651 as a result of higher amplitude ratio and cycle ratio was found higher than 7075-T651.

The CGR in 3.5% NaCl environment was found accelerated. The CGR enhanced with the increase in amplitude ratio and cycle ratio^{21, 9)}. At higher amplitude ratios the corrosive environment causes a larger increase in CGR.

In addition to the test variables discussed in this paper, other factors have also been investigated such as microstructure, specimen thickness, location of the specimen through the thickness, orientation and texture influence the fatigue and corrosion fatigue crack growth rates. The usage parameters of an aircraft and fleet will provide a volume of

variables effects of which on the fatigue and corrosion fatigue behavior of aluminum alloys is not known. Therefore, more research needs to be undertaken to generate and compile data that can be used in probabilistic data synthesis in order to conduct the repair and determine further usage of an aircraft or fleet.

4 CONCLUSION

The effect of test parameters on the corrosion fatigue crack growth behavior of aircraft structural materials has been examined in this paper. It has been shown that the presence of corrosive environment increases the CGR in all the three major alloy groups used in aircraft namely aluminum alloys, titanium alloys and steel. Numerous test parameters that influence the CGR are as follows:

1. an increase in the stress ratio increased the CGR in aluminum alloys, titanium alloys and steel, where the increase in CGR was seen at the lower and higher ranges of mode I ΔK , which enhanced further with the corrosive environment,
2. as the frequency reduced the crack growth rates increased in most materials, the rate of increase in CGR was found more severe with the corrosive environment,
3. at lower frequency ranges mild environments produced similar CGR that of more aggressive environment,
4. sub-surface cracking was observed as a major failure mechanism in titanium alloys under SCC,
5. all materials examined in this paper showed a level of CGR in SCC tests, thereby, a

- range of mode I ΔK was not found existing for these materials,
6. specimen thickness, orientation and the location from where the specimen was machined produced a different CGR,
 7. with the increase in cycle ratio and amplitude ratio the CGR increased in four aluminum alloys, the CGR increased further as the environment became more aggressive i.e., in 3.5% NaCl solution, and
 8. there are several other parameters which are not usually investigated e.g., texture, grain size, percentage of constituent particles and their sizes etc., produce different CGR in the materials examined in this paper.

More work is recommended to generate and compile data that can be synthesized in the probabilistic analysis pertaining to growth rate estimations and next inspection interval determinations for aircraft/fleets.

5 REFERENCES:

1. A. Hartman, *Int. J. Fracture Mech.* 1, (1965), 167.
2. M. Pourbaix, *Atlas of electrochemical equilibrium diagrams in aqueous solutions* NACE, (1966).
3. R. Ambat, and E. S. Dwarakadasa, *British Corrosion Journal*, 38, 2, (1993), 142.
4. F. J. Bradshaw, and C. Wheeler, *Applied Mats. Res.* 5, (1966), 112.
5. D. W. Hoepfner, and W. S. Hyler, *Materials Res. and Standards*, 6, 12, (1966), 599.
6. D. E. Petit, J. T. Ryder, W. E. Krupp, and D. W. Hoepfner, *AFML-TR-1974-183* (1974).
7. D. W. Hoepfner, *Corrosion fatigue : chemistry, mechanics and microstructure*, NACE-2, (1971), 3.
8. W. E. Krupp, D. W. Hoepfner, and E. K. Walker, *NACE-2*, (1971), 468.

9. D.W. Hoepfner and T. Goswami, Unpublished work, Quality and Integrity Design Integrity Center, University of Utah, (1994).
10. G. R. Irwin, Syracuse University Research Institute, (1960), IV-63.
11. S. R. Novak, and S. T. Rolfe, *J. of Mater.* 4, (1969), 701.
12. J. A. Feeney, J.C. McMillan, and R. P. Wei, *Met. Trans.* 1, (1970), 1741.
13. M.R. Achter, *Scripta Met.* 2, (1968), 525.
14. L.R. Hall, R.W. Finger, and F.W. Spurr, AFML-TR-1973-204, (1973).
15. D. S. Cowgill, J. S. Fritzen, S. Krystkowiak, and K. E. Weber, ASTM ARPA Symposium on stress corrosion and corrosion principles, Atlanta, (1968).
16. G. R. Yoder, L. A. Cooley, and T. W. Crooker, *Eng. Fracture Mech.* 11, (1979), 805.
17. K. R. Kondas, T. W. Crooker, and C. M. Gilmore, *Eng. Frac. Mech.* 7, (1975), 641.
18. G. R. Yoder, L. A. Cooley, and T. W. Crooker, *Met. Trans.* 8A, (1977), 1737.
19. B. E. Powell, T. V. Duggan, and R. Jeal, *Int. J. of Fatigue*, 4, (1982), 4.
20. A. D. Paulson, Ph.D. Dissertation University of Utah, Department of Mechanical Engineering (1993).
21. A. D. Paulson, and D. W. Hoepfner, Durability and Structural Integrity of Airframes, 17th ICAF Symposium, EMAS 2, (1993), 1099.

